Coupled oscillations in the aeroacoustics of a Katana blade

Michel Roger

Ecole Centrale de Lyon, 36 Avenue Guy de Collongue, Centre Acoustique, 69134 Ecully, France
michel.roger@ec-lyon.fr

The paper investigates the sound of a Katana blade, as a special case of aerodynamic body in a flow. The acoustic signature involves a relatively low-frequency sound due to the vortex-shedding in the blade wake, and high-frequency tones due either to shear-layer oscillations over the grooves or to laminar instabilities in the boundary layers. All features and their variations with flow speed and angle of attack are investigated experimentally. Finally two analytical models of the vortex-shedding noise are successfully tested against the measurements. The different oscillatory motions are found to be coupled but the coupling mechanism still remains to be understood.
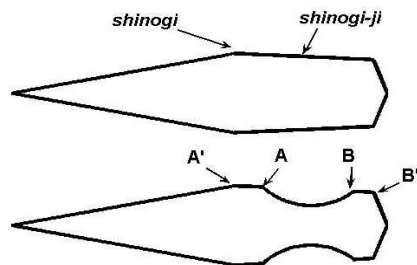
Figure 1: *Katana-blade profiles investigated in the present study, without groove (top) and with groove between edges* A *and* B *(bottom).*
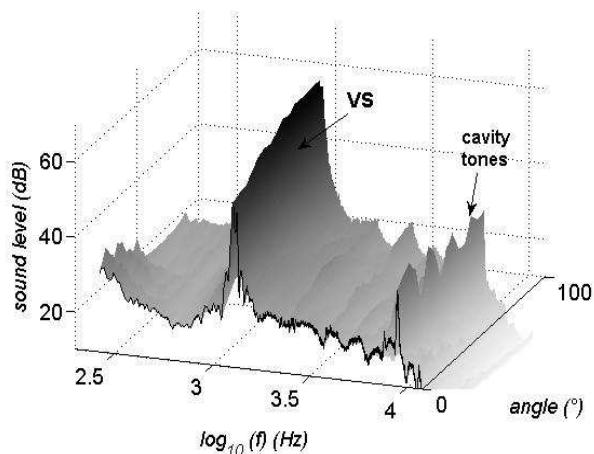
Figure 2: *Typical acoustic signature of a real Katana blade in wind-tunnel testing, in the frequency-radiation angle plane. Profile with symmetric grooves. Flow speed* $24\,m/s$.

1 Introduction

Katana is the name of the traditional single-edge, slightly curved sword used in Japanese martial arts. When the Katana is handled for cutting, the blade is expectedly moved through the air at a relatively high speed and a hiss or hushing sound can be heard. This sound depends on the angle of attack, the flow speed and the blade-profile design.

The basic cross-section of a Katana blade involves a single cutting edge and a blunt back-edge similar to the base of a ballistic projectile (Fig. 1). From the aerodynamical point of view the cutting edge equivalent to a leading edge and the base equivalent to a thick or blunted trailing-edge. The traditional design involves a middle ridge or *Shinogi*. The bluntness is responsible

for the formation of a von Kármán vortex street in the wake of the blade. The corresponding acoustic signature is referred to as the vortex-shedding sound later on in the paper. It is well dominant on the typical spectra plotted in Fig. 2 as a function of emission angle, where it is labelled **VS**. The results concern a real Katana blade inserted between side-plates in the nozzle exit of the anechoic open-jet wind tunnel of Ecole Centrale de Lyon. The chord length is $3\,cm$ and the blade section is the profile of Fig.1-bottom. The vortex-shedding sound is heard around $960\,Hz$. Furthermore, some Katanas are designed with so-called 'blood-grooves' along the flat surface behind the *shinogi*, named *shinogi-ji* (Fig. 1-bottom). The actual reason for these grooves is a weight reduction at constant structural strength. The grooves are equivalent to two-dimensional cavities under a grazing flow. Therefore cavity tones are generated, due to the instabilities of the free shear layers detaching from the upstream edges (A) of the grooves and impinging on the downstream edges (B), as generally observed for shallow cavities [1]. This second mechanism will be referred to as the groove-tones or cavity-tones in the paper. It is responsible for the high-frequency sound observed in Fig.2 around 6 to $8\,kHz$. As seen later on, designs not including grooves (Fig. 1-top) have another high-frequency signature, due to laminar instabilities of the boundary layers (Tollmien-Schlichting waves). This makes the Katana blade a very rich example of sound-generating body in aeroacoustics, not previously addressed to the author's knowledge.

2 Experimental Results

The rectangular mock-up used in this study is twice the size of the real Katana of Fig. 2. The chord length is $6\,cm$ and the thickness of the back-edge $1\,cm$. The corresponding chord-based Reynolds number ranges from $40,000$ to $120,000$. The results of sections 2.1 and 2.2 are obtained for the Katana with grooves and the effect of filling one or both grooves is discussed in section 2.3.

2.1 Effect of Flow Speed

The sound measured at 90° to the the flow direction for a blade at zero angle of attack is plotted here in Fig. 3 as a function of oncoming flow speed, by making the frequency non-dimensional with the Strouhal number based on the flow speed and the base thickness h. As expected the vortex-shedding frequency and its harmonics are found proportional to the flow speed. The fundamental Strouhal number is found to be 0.21, close to the classical value for a cylinder or a bluff body in a flow. The first harmonic at twice this value is not seen,

because it does not radiate in the direction of the microphone. In contrast the second harmonic has the same basic directivity as the fundamental tone and is clearly observed for a reduced frequency of 0.63. More generally, odd harmonic orders are expected in the acoustic signature. However the third horizontal trace from the bottom in Fig. 3 is significantly too low to be the higher vortex-shedding harmonic number 5. Another typical acoustic signature is featured by the relatively high-frequency traces.
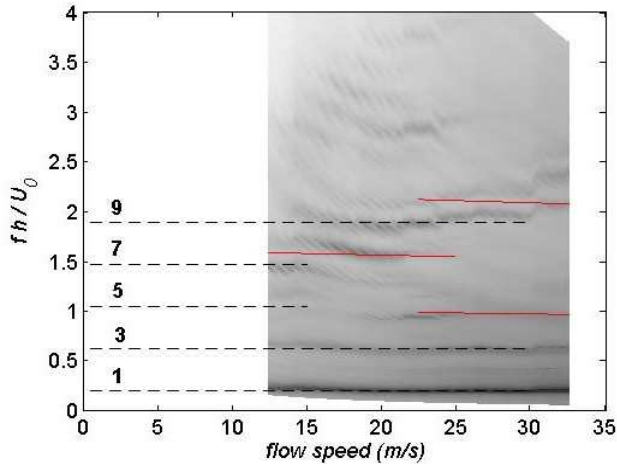
Figure 3: *Strouhal number as a function of flow speed. Mock-up of Fig. 1-bottom. Harmonics of the vortex-shedding and cavity tone orders pointed by lines for convenience.*

The origin of the sound at higher frequencies is better sought in the literature on shallow cavities under a grazing flow [1]. Assuming that the self-sustained oscillations over the cavity involve acoustic back-reaction between both edges noted A and B, the feedback loop analysis leads to simple expressions for the tonal frequencies. Let U_c be the convection speed of the instabilities in the cavity shear layer, typically 0.65 times the external flow speed U_0, and L the feedback distance between A and B. A frequency is amplified if the convection time of the instability wave from A to B plus the propagation time upstream from B to A equals a multiple of the period of oscillations, accounting for a phase-shift at the sound emission. The phase shift has been evaluated as a quarter period for the corner of a rectangular cavity and the same indicative value is retained here, leading to some uncertainty. Introducing the Mach number $M_0 = U_0/c_0$, the selective condition for the tones reads:

$$S_n = \frac{f\,h}{U_0} = \frac{h}{L}\frac{f\,L}{U_0} = \frac{h}{L}\frac{n-0.25}{(U_0/U_c) + M_0/(1-M_0)} \tag{1}$$

The modes 2 to 4 deduced from this equation are plotted in Fig. 3 (mode 1 is often not observed in cavity experiments, especially at low Mach numbers). The back-edge thickness h is used as a length scale instead of the cavity length L in order to make all non-dimensional frequencies comparable on the same plot. Despite some expected inaccuracy from the lack of precise informa-
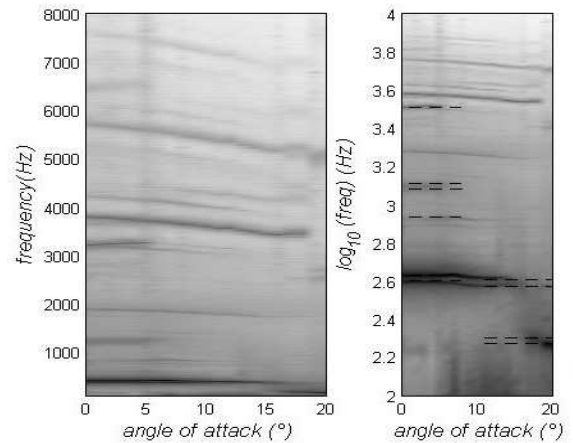
Figure 4: *Variations of model-blade tones with the angle of attack at constant flow speed $20\,m/s$. Two-dimensional mock-up. Harmonics of the vortex-shedding Strouhal number and cavity tones pointed for convenience.*

tion on the shear-layer instabilities, the results suggest that the third trace from the bottom is rather related to the cavity mode $n = 2$ (Strouhal number around 1). This trace is observed only at high speed in the experiment. In contrast another trace corresponding to the mode $n = 3$ locally dominates at lower speed (Strouhal number around 1.6). Higher harmonics of the vortex-shedding frequency are not probable because intermediate harmonics would be generated too, which do not appear on the plot. This confirms that the high-frequency acoustic signature is due to the grooves. The sinuous trace between the lines of cavity modes $n = 3, 4$ is less clear and approximately corresponds to the harmonic of order 9 of the vortex-shedding frequency. The occurence of this harmonic is quite surprising because it corresponds to very tiny details of the oscillatory motion associated with the vortex shedding. The proposed explanation is that this sound is again due to the cavity but that its description excapes the scope of the usual feedback analysis of equation (1) because the self-sustained oscillations in the cavity are partially triggered by the vortex-shedding. Two oscillating motions occuring in the same time are known to modulate each other and this should happen in the present case with the vortex shedding and the cavity oscillations. This interpretation is suggested by the multiple secondary horizontal fringes of Fig. 3 (essentially between 15 and 25 m/s), which are separated by a regular vertical shift of about 0.21 in Strouhal number.

2.2 Effect of the Angle of Attack

The net effect of varying the angle of attack on the far-field measurements is shown in Fig. 4 for a relatively high speed of $20\,m/s$ and a wide range of possible angles of attack up to $20°$ with respect to the usual handling of a Katana. For moderate angles $\alpha < 8°$, the vortex-shedding signature is nearly unaffected when compared to the reference case at zero angle of attack.

At higher angles, typically above $\alpha = 10°$, the fundamental vortex-shedding frequency shifts to lower values (note that the peak is split into two narrower quasi-tonal peaks at close values of the Strouhal number 0.2 and 0.215). In the same time the higher harmonics are not observed anymore. Moreover, at even higher angle of attack, around $\alpha = 15°$, the vortex-shedding sound suddenly drops, and reappears at half the usual frequency. This jump corresponds to a stalled flow over the blade with a recirculation bubble, leading to larger-scale motion in the wake. Alternatively the frequencies attributed to the grooves vary continuously with the angle of attack, the lower-order tones only vanishing at the highest values. This behaviour difference confirms the interpretation and classification previously proposed in terms of vortex-shedding tones and groove tones. Both contributions are clearly recognised as different in the range of moderate angles of attack, depending on either the traces on the plot of Fig. 4 are horizontal or not. For instance, the tone starting around $2000\,Hz$ on the left-hand side plot is attributed to the cavity and is definitely not to be confused with a vortex-shedding harmonic.

2.3 Filled-groove configurations

In this section the same Katana blade profile with filled grooves is investigated. First filling both grooves is equivalent to investigate the blade design of Fig. 1-top with a flat, regular *shinogi-ji*. In that case the groove tones do not exist but are replaced by another high-frequency signature, plotted for comparison in the Fig. 5-right. The tones are attributed to Tollmien-Schlichting (TS) instability waves characteristic of oscillating laminar turbulent boundary layers. The mechanism for the TS-wave radiation is similar to the oscillations over a shallow cavity. Point A' (Fig. 1-top) is the onset of instabilities in the laminar boundary layer due to the *shinogi* and point B' at the base corner causes scattering of the instability waves as sound. Equation (1) is then valid, provided that the length of the acoustic feedback loop is changed, and explains why the fequencies are slightly lower than with the grooves. A modification of the spectral structure of the vortex-shedding sound is also observed in the presence of TS-wave radiation, as seen by inspection of Fig.5-right at low angles of attack. The vortex-shedding peak is split into two or three, different from its spectral shape in other configurations. This shows evidence of a specific coupling between the vortex-shedding sound and the TS-wave radiation, still to be understood.

The last configuration addressed in this paper is a Katana blade with a groove on one side only. In this case the asymmetry of the cross-section makes different noise features expectable depending on the angle of attack. The effect of this parameter on the noise radiated at $90°$ to the flow direction for the given flow speed $20\,m/s$ is summarised in Fig. 5. The angle of attack is varied from $-20°$ to $+20°$. The side of the groove is a pressure side for positive values and a suction side for negative values.

Significantly less sound is radiated when the groove is on the suction side of the inclined blade. More pre-
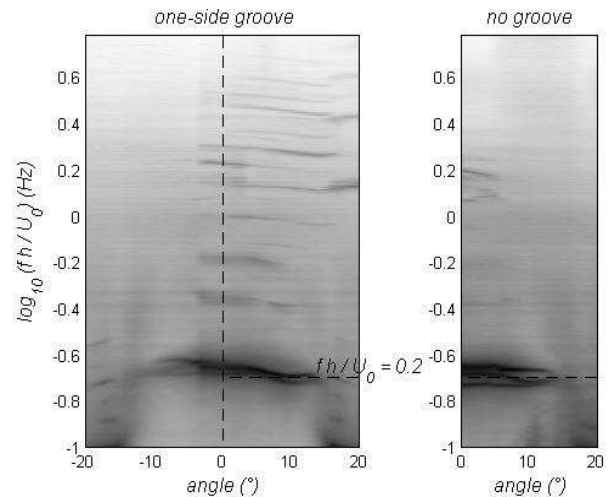
Figure 5: *Left plot: angle-frequency map of the acoustic signature of the model Katana blade with a single groove. Groove on the pressure side for positive angles and on the suction side for negative angles. Right plot: same map for the Katana with no groove.*

cisely, sound is radiated symmetrically for angles of attack between $-4°$ and $+4°$. In accordance with the general features of the aerodynamic noise radiated by airfoils, this means that no noticeable change occurs in the flow around the Katana blade within the range of small angles of attack. In contrast, the asymmetry at high angles of attack means that the flow features are fundamentally different depending on the groove is under-pressured or over-pressured. The high-frequency sounds attributed to the groove tones disappear at significant angle of attack when the groove is on the suction side because the flow separates from the middle ridge and the corners of the groove escape the flow impingement. More surprising is the relative vortex-shedding sound extinction when the groove is on the suction side for an extended range of angles of attack between $-6°$ and $-14°$. At very high angles of attack, typically between $15°$ and $20°$, the stalled flow regime over the Katana blade is recovered and the map is symmetric again. The extinction regime of the vortex-shedding sound suggests that a groove closely upstream of a thick trailing-edge could be a reduction mean in other applications of industrial interest.

3 Analytical Predictions

3.1 Simplified Model

Despite the lack of precise information about the flow features, a simplified vortex-shedding noise model is described in this section, based on previously published formulations dealing with compact bluff bodies in a flow. The vortex shedding occurs at the Strouhal frequency $f_0 = 0.2\,U_0/h$ and the Katana relative thickness at back edge is $h/c = 1/6$. Therefore the Helmholtz number based on the chord of the cross-section $kc = 2\pi\,f_0\,c/c_0 \simeq 2.4\pi\,M_0$ introducing the mach number $M_0 = U_0/c_0$,

is found much smaller than 1. This means that a cross-section of the blade radiates in the same way as a compact dipole and can be modelled as such. The strength of the equivalent dipole can be estimated by the method proposed by Fukano *et al.* for the broadband trailing-edge noise of a fan blade due to random vortex-shedding [3]. The unsteady lift induced on the body is related to the variations of circulation in the wake. The circulation of a near-wake vortex is first estimated as $U_0 h$ for a well-structured vortex formation close to the corners of the back edge. This leads to a simple model of the unsteady lift coefficient induced on the blade per unit span as $C_L \simeq 2 \, (h/c) \, e^{-i \, 2\pi \, f_0 t}$. In a second step, a consistent prediction of the far-field intensity around the Strouhal frequency is deduced from the same analysis as made by Goldstein for a circular cylinder, introducing a spanwise correlation length to account for the statistical properties of the distributed vortex shedding [4]. A Gaussian correlation coefficient with a spanwise length scale ℓ_0 is assumed. Other available investigations on flat plates of large chord-to-thickness ratio suggest that $\ell_0 \simeq 7 \, h$ [2], so this value is taken for granted in the present case, even though it is somewhat larger than the value for a cylinder. At the very low Mach number of interest for which $M_0 \ll 1$, the peak intensity of vortex-shedding sound is expressed as

$$I = \frac{\sqrt{2\pi} \, (C_L \, S_t)^2 \, \rho_0 \, U_0^6 \, L \, \ell_0}{32 \, c_0^3 \, R^2} \, \sin^2 \theta \qquad (2)$$

ρ_0 and c_0 being the air density and sound speed, L the span length, (R, θ) the observer distance and angular location with respect to the direction of the oncoming flow, for an origin of coordinates taken at the blade center point. Equation (2) predicts the increase of sound intensity with the sixth power of the flow speed and the two-lobed directivity pattern, typical of compact dipoles. The U_0^6 scaling law is first tested against the measurements in Fig. 6. For this the measured spectra have been integrated over a narrow frequency range including the peak signature of the vortex shedding. A reasonable agreement is found, even though the actual sound is slightly underpredicted with the present assumptions. A more accurate estimation would require for instance flow simulations in the near wake which are not available here. As expected, the measurements globally follow the sixth-power law, with a faster increase at higher speeds, above $20 \, m/s$.

The model directivity of the sound will be discussed in the next section.

3.2 Spectral Model

Even though simple by virtue of its compactness, the presently investigated Katana blade can be treated by more general formulations as a special test case. The predictions made in this section are based on the analytical model of the vortex-shedding noise from a thin rigid flat-plate body with a blunted trailing edge proposed by Roger *et al.* [2]. Since this less restrictive model deals with an arbitrary chord length, the corresponding calculations will be said non-compact here for convenience. Furthermore it is aimed at reproducing the spectral content of the vortex-shedding noise and as such it is more
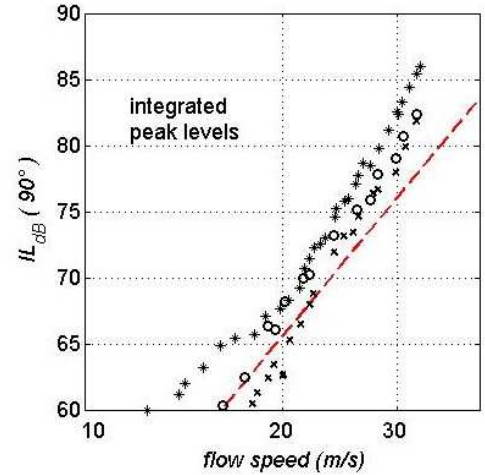
Figure 6: *Scaling law for the vortex-shedding noise of the model Katana blade. Dashed line: U_0^6-law according to eq. (2). Symbols: measurements with integration range from $0.7 f_0$ to $1.5 f_0$.*

demanding of input data. The unsteady lift induced on the body by the shed vortices is evaluated by resorting to an inverse Sears' problem, according to an extension of Amiet's solving procedure in which the convection speed of the vortices U_c in the wake is considered different from the main-flow speed U_0. In a second step the far-field sound is evaluated from the unsteady lift according to the acoustic analogy. Details of the model are not given here. The PSD of the far-field pressure in the mid-span plane reads

$$S_{pp}(\vec{x}, \omega) = \left(\frac{\rho_0 \, k \, c \, x_2 \, U_0}{2 \, S_0^2} \right)^2 \frac{L}{2} \, S_{ww}(\omega) \, l_y(\omega) \, |I_{VK}|^2 \qquad (3)$$

where ρ_0 is the fluid density, c the chord length, L the spanwise extent, k the acoustic wavenumber, x_2 the co-ordinate normal to the chord line, with the origin of coordinates at the trailing-edge center. $S_{ww}(\omega)$ stands for the spectrum of the normal velocity oscillations in the near wake and $l_y(\omega)$ for the corresponding spanwise correlation length. At the very low Mach numbers of interest, S_0 can be assimilated to the geometrical distance to the observer and $x_2/S_0 = \sin\theta$, θ being the angle from the downstream direction. The aeroacoustic response function I_{VK} is derived analytically as

$$I_{VK} = -\frac{(1+i)}{\pi \, k_1^*} \left\{ \sqrt{\frac{\Theta_1}{\Theta_1 - \Theta_2}} \, E^* \left[2 \, (\Theta_1 - \Theta_2) \right] \right. \qquad (4)$$

$$\left. \times \left(1 - \frac{\bar{k}_1 - \bar{k}_0}{\Theta_2} \right) + (\bar{k}_1 - \bar{k}_0) \frac{e^{2 \, i \, \Theta_2}}{\Theta_2} \, E^* \left[2 \, \Theta_1 \right] \right\}$$

with

$$E^*(\xi) = \int_0^\xi \frac{e^{-i \, t}}{\sqrt{2 \, \pi \, t}} \, dt \qquad \Theta_1 = \bar{k}_1 + \bar{\mu} \, (1 + M_0)$$

$$\Theta_2 = \bar{k}_1 - \bar{\mu} \left(\frac{x_1}{M_0} - M_0 \right)$$

$\bar{\mu} = kc/(2\beta^2)$, $k_0 = \omega/U_0$ and $k_1 = \omega/U_c$, $k_1^* = \bar{k}_1 [1 - M_0^2(1 - k_0/k_1)^2]^{1/2}$ and the bar on a wavenumber corresponds to a multiplication by $c/2$. The spanwise correlation length typical of the vortex shedding can be written as $l_y(\omega) = \sqrt{\pi/2}\,\Lambda(\omega)$, with $\Lambda(\omega) = \Lambda_0\, e^{-\alpha\,|\omega-\omega_0|}$, α being an adjustable constant, around $0.012/(2\pi)$ for $U_0 = 20\,m/s$. In the same way numerical simulations and measurements performed on flat-plate configurations involving a rectangular back-edge lead to the non-dimensional velocity spectrum $10\,\log_{10}\,(S_{ww}^0/U_0) = -27 - 500|S_t - 0.2|$. Such a model reproduces the moderate spectral speading around the Strouhal frequency. The last needed parameter for analytical calculations is the mean convection speed U_c. It has been found $0.56\,U_0$ in the near wake in the computations, and around $0.6\,U_0$ according to some hot-wire measurements. The model
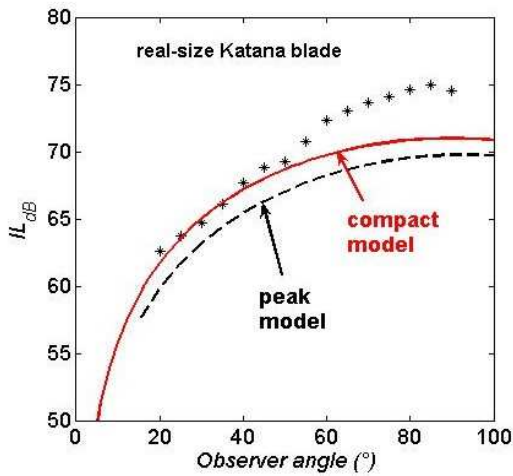
Figure 7: *Directivity of the true Katana blade in wind-tunnel, with integration range from $0.7f_0$ to $1.5f_0$. Predictions: dipole patterns according to eq. (2) (cont. line) and eq. (2) (dashed line).*

Figure 8: *Frequency-angle plot of the sound of the true Katana blade. Prediction from eq. (2) versus measurements.*

directivity from eq. (2) is plotted in Fig. 7 where it is compared to the measurements for the true Katana blade (scale 1) in the mid-span plane. A relatively good agreement is obtained, with discrepancies part attributed to spurious scattering at the edges of the wind-tunnel nozzle. The same underprediction at 90° as in Fig. 6 is also found. The spectrum and directivity of the vortex-shedding sound as predicted by the non-compact model are also compared to the measurements for the true Katana of section 1 in Fig. 8, where the frequency range has been focussed around the Strouhal frequency. With the assumptions taken from previous flat-plate investigations, the spectral broadening is fairly well reproduced but the amplitude remains underpredicted by a couple of decibels. The global directivity also reported in Fig. 7 is nearly the same as with the compact model, as expected in view of the parameters.

4 Conclusion

The sound of a Katana blade combines a low-frequency vortex-shedding sound due to the thickness of the blade at the back edge, and a high-frequency series of tones due to either groove oscillations or TS waves, depending on the blade design. The variations of the sound with flow speed and angle of attack have been analysed and could be used to check the practical handling of the Katana. Furthermore the Katana is a test case on which available vortex-shedding sound models are successfully tested. The coupling between the different sound features still remains to bo investigated.

Acknowledgements

References

[1] Rockwell, D. & Naudascher, E., "Review - Self-Sustained Oscillations of Flow Past Cavities", Trans. ASME, vol. 100 (1978)

[2] Roger M., Moreau S. & Guédel A., "Vortex-Shedding Noise and Potential-Interaction Noise modeling by a Reversed Sears' Problem", 12th *AIAA/CEAS Aeroacoustics Conference*, paper 2006-2607, Cambridge, MA, 2006

[3] Fukano T., Kodama Y. & Senoo Y., "Noise generated by low-pressure axial flow fans. I: modeling of the turbulent noise", *J. Sound and Vib.*, 50 (1), pp. 63–74, 1977.

[4] Goldstein M.E., "Aeroacoustics", *McGraw-Hill New-York*, 1976.